

1 **Interannual variability in lower trophic levels on the Alaskan Shelf**

2 *Sonia D. Batten¹, Dionysios E. Raitsos², Seth Danielson³, Russell Hopcroft³, Kenneth Coyle³
3 and Abigail McQuatters-Gollop⁴

4 ^{1*} Sir Alister Hardy Foundation for Ocean Science, c/o 4737 Vista View Cr, Nanaimo, BC, V9V
5 1N8, Canada. soba@sahfos.ac.uk

6 ² Plymouth Marine Laboratory, Prospect Place, The Hoe, Plymouth, PL1 3DH, United Kingdom

7 ³ Institute of Marine Science, 120 O'Neill, P.O. Box 757220, University of Alaska Fairbanks,
8 Fairbanks, AK 99775-7220, USA.

9 ⁴ Centre for Marine and Conservation Policy, Plymouth University, Drake Circus, Plymouth,
10 PL4 8AA, UK.

11

12 **Abstract**

13 This study describes results from the first 16 years of the Continuous Plankton Recorder (CPR)
14 program that has sampled the lower trophic levels (restricted to larger, hard-shelled
15 phytoplankton and robust zooplankton taxa) on the Alaskan shelf. Sampling took place along
16 transects from the open ocean across the shelf (to the entrance to Prince William Sound from
17 2000 to 2003 and into Cook Inlet from 2004 to 2015) to provide plankton abundance data, spring
18 through autumn of each year. We document interannual variability in concentration and
19 composition of the plankton community of the region over this time period. At least in part and
20 through correlative relationships, this can be attributed to changes in the physical environment,
21 particularly direct and indirect effects of temperature. For example; spring mixed layer depth is
22 shown to influence the timing of the spring diatom peak and warmer years are biased towards
23 smaller copepod species. A significant positive relationship between temperature, diatom
24 abundance and zooplankton biomass existed from 2000 to 2013 but was not present in the warm
25 years of 2014 and 2015. These results suggest that anomalous warming events, such as the “heat
26 wave” of 2014-2015, could fundamentally influence typical lower trophic level patterns, possibly
27 altering trophic interactions.

28

29 **Key Words**

30 Cook Inlet, Alaskan Shelf, Continuous Plankton Recorder, Zooplankton, Phytoplankton.

31

32 **Highlights**

33

34 **1. Introduction**

35 The south Alaskan Shelf region that encompasses the large inlets of Cook Inlet (CI) and Prince
36 William Sound (PWS) and the outer shelf of the northern Gulf of Alaska is a productive,
37 dynamic, subarctic shelf system supporting numerous valued marine resources such as
38 commercially-harvestable fish (e.g. herring, salmon, groundfish), large marine mammals (e.g.
39 belugas, humpback whales), and seabirds. Lower trophic level productivity underpins this
40 ecosystem but our understanding of plankton variability in this region is still somewhat limited.

41 It is recognized now that forcing of marine ecosystems occurs at multiple temporal and spatial
42 scales. It is challenging to attempt to understand the impacts of climate change on marine
43 organisms and detect trends in data when there is high interannual variability in both the physical
44 forcing and biological responses. For example, restoration projects for injured resources
45 following the Exxon Valdez oil spill in PWS in 1989 have struggled with teasing apart the
46 impacts of this one-off catastrophic event from naturally-induced variability (EVOS Trustee
47 Council, 2010). Natural, rather than human-related, processes known to influence this region are
48 numerous. For example, on seasonal and interannual time scales the strength of the Alaskan shelf
49 and Alaskan Coastal currents are mediated by freshwater run-off and winds (Royer, 1979;
50 Stabeno et al., 2004; Weingartner et al., 2005), persistent coastal downwelling in contrast to most
51 eastern Pacific boundary regions, and eddy-mediated cross-shelf transport of organisms and
52 nutrients (Okkonen et al., 2003; Ladd et al., 2005). More quasi-decadal time scale influences are
53 the change in sign of the Pacific Decadal Oscillation (PDO), which is based on the analysis of
54 Mantua et al. (1997) and is the first mode of ocean surface temperature variability in the North
55 Pacific Ocean. Historically it has been a good indicator of weather patterns that persist for a
56 decade or more but has more recently been switching state approximately every 5 years. Positive
57 (negative) PDO values are associated with warmer (cooler) than normal conditions in the NE
58 Pacific. A second medium time-scale influence is the North Pacific Gyre Oscillation (NPGO), a
59 climate pattern that emerges as the second dominant mode of sea surface height variability in the
60 Northeast Pacific Ocean (Di Lorenzo et al., 2008, <http://www.o3d.org/npgo/>). When the NPGO
61 index is positive the westerly winds over the eastern North Pacific are often stronger than
62 normal, influencing the circulation processes. Moderate to strong El Niño and La Niña events are
63 also evident on the Alaskan Shelf (Weingartner et al., 2002). Regime shifts, which may be

64 triggered by the climate processes described above, have periodically occurred with lower
65 frequency, such as the 1976 shift which changed Alaskan fisheries from shrimp to fish
66 dominated (Francis and Hare, 1994). More recently, anomalous warming across a wide expanse
67 of the Northeast Pacific occurred late in 2013 and persisted through 2014 (Bond et al, 2015).
68 Nicknamed “the Blob” and succeeded by a strong El Nino in 2015, the Alaskan shelf has been
69 influenced by these strong warming events for at least two consecutive years (DiLorenzo and
70 Mantua, 2016).

71 With short generation times, limited mobility and lack of a commercial harvest, plankton often
72 respond to changes in their environment more rapidly and less ambiguously than higher trophic
73 levels, so that a relatively short time series of plankton information can provide insights into the
74 responses of the shelf ecosystem to some of the processes described above. Primary productivity
75 is strongly seasonal in this region, owing primarily to the relatively high latitude and low light
76 levels in winter. Mueter et al. (2009) report that although there are clear peaks in satellite-derived
77 chlorophyll-*a* levels in spring and autumn (owing to the spring bloom and replenishment of
78 nutrients by autumn storms respectively) there is in fact a single broad peak of productivity in the
79 Gulf of Alaska through summer that is heavily grazed by zooplankton and so results in low
80 phytoplankton standing stocks in summer. There has been significant interannual variability in
81 chlorophyll-*a* concentrations over the previous decade and more, with positive anomalies in
82 years with reduced cloud cover, lower SST and reduced downwelling-favourable winds (Waite
83 and Mueter, 2013). These observations do not necessarily represent variability in primary
84 productivity but may suggest that strong cyclonic circulation does not favour high chlorophyll-*a*
85 concentrations throughout the Gulf of Alaska.

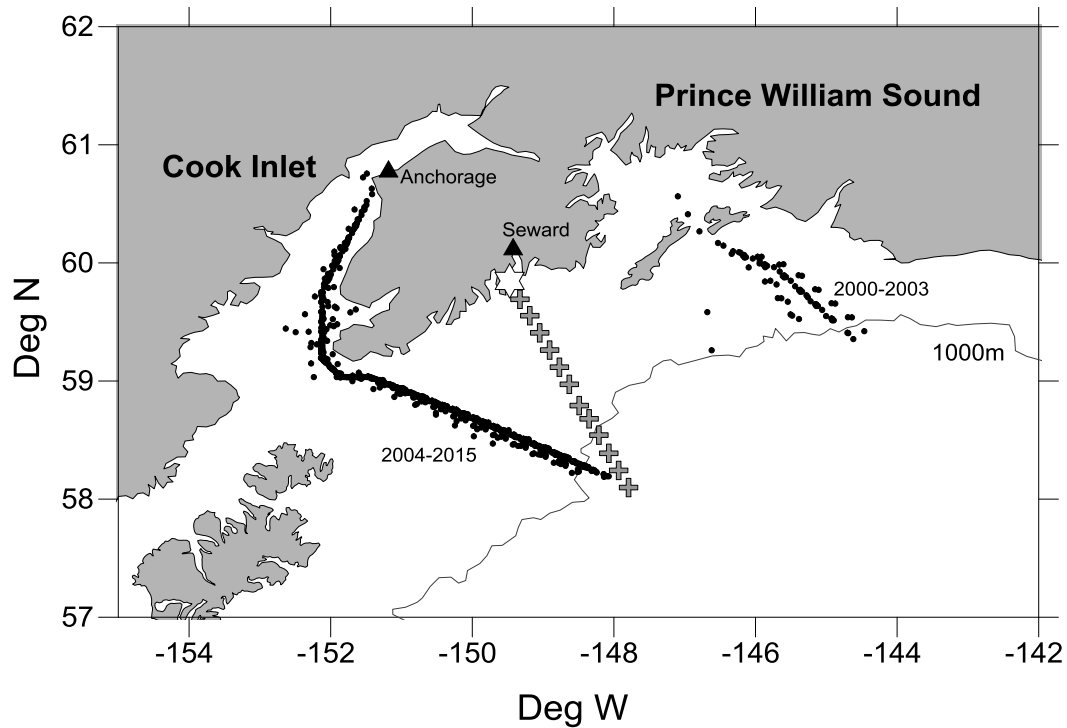
86 Previous studies of zooplankton on the shelf (Coyle and Pinchuk, 2003) and in PWS (Cooney et
87 al., 2001) suggest a strong seasonal community dominated by copepods (with significant
88 contributions from other taxa such as cnidarians on the shelf, euphausiids, pteropods and
89 larvaceans seasonally in PWS). While small-medium sized copepod species dominated in terms
90 of abundance at all times of year, the biomass in spring and early summer was dominated by
91 larger copepods that spend the winter in diapause at depth. Negative salinity anomalies, followed
92 by temperature, were the strongest influencers of the zooplankton community (Coyle and
93 Pinchuk, 2003).

94 The Continuous Plankton Recorder (CPR) was designed to be towed behind commercial ships
95 and to sample plankton from near surface waters over large spatial scales (Batten et al., 2003a).
96 This study describes results from the first 16 years of the Continuous Plankton Recorder (CPR)
97 program that has sampled the lower trophic levels of the south-central Alaska Shelf, on a
98 seasonal basis from spring to autumn. Although restricted to larger, hard-shelled phytoplankton
99 and robust zooplankton taxa, this dataset is complementary to previous studies which have been
100 more geographically focussed but with reduced temporal coverage. The CPR data are now
101 sufficient to examine the interannual variability of the plankton populations with respect to
102 changing oceanographic conditions of the region.

103 **2. Methods**

104 **2.1 Sampling**

105 The CPR was towed behind a volunteer commercial vessel making the sampling cost-effective,
106 but with limited ability to control the timing of the sampling and no ability to determine the
107 transect position. The original transect operated from 2000 between ports in California, USA and
108 PWS, with sampling normally stopping at Hinchinbrook Entrance. Owing to changes in shipping
109 activities the transect was changed in 2004 to a route from the mouth of Juan de Fuca Strait (at
110 the border of British Columbia, Canada, and Washington State, USA) to Anchorage, with
111 sampling normally stopping in CI between about 59-60°N (Fig 1). Start and end of sampling was
112 always at the discretion of the vessel's Captain. The second transect was remarkably consistent
113 with almost identical transect positions each month, particularly at the northern end with which
114 this study is concerned. Frequency of sampling was at approximately monthly intervals in most
115 years (occasionally two transects occurred in one calendar month), commencing in about April
116 and ending in about September, but occasionally sampling March and October (Table 1).
117 Mechanical failures, human error and marine debris mean that in any one year, one or two
118 months may have reduced, or no, data available. In summary, while the available data have gaps,
119 they represent a sufficiently lengthy and spatially expansive time series of seasonal data with
120 which to examine lower trophic level variability in this region.



121

122

123

124

125

126

127

128

129 Table 1. Months for which data were available in each year.

130

Transect	Year	Mar	Apr	May	Jun	Jul	Aug	Sep	Oct
PWS	2000	X	X			X	X		
PWS	2001		X	X	X			X	
PWS	2002		X			X			X
PWS	2003			X			X		
Cook Inlet	2004	X	X		X	X	X		
Cook Inlet	2005		X	X		X	X		
Cook Inlet	2006	X	X			X	X	X	X
Cook Inlet	2007		X		X		X	X	
Cook Inlet	2008				X			X	
Cook Inlet	2009		X	X	X		X		
Cook Inlet	2010		X			X		X	
Cook Inlet	2011		X	X		X	X	X	

Cook Inlet	2012		X	X	X	X		X	X
Cook Inlet	2013		X	X	X	X	X	X	
Cook Inlet	2014	X	X	X	X	X	X		
Cook Inlet	2015		X		X		X	X	

131

132

133 A summary is given here but for a full description of the CPR instrument and sampling protocols
 134 see Batten et al. (2003a) and see Richardson et al. (2006) for data analysis methods.

135 The CPR was towed in the wake of the ship at a depth of about 7m. Water and plankton enter the
 136 front of the CPR through a small square aperture (sides of 1.27 cm), pass along a tunnel, and
 137 then through the silk filtering mesh (with a mesh size of 270 μm) which retains the plankton and
 138 allows the water to exit at the back of the machine. The movement of the CPR through the water
 139 turns an external propeller which, via a drive shaft and gear-box, moves the filtering mesh across
 140 the tunnel at a rate of approximately 10 cm per 18.5 km of tow. As the filtering mesh leaves the
 141 tunnel it is covered by a second band of mesh so that the plankton are sandwiched between these
 142 two layers. This mesh and plankton sandwich is then wound into a storage chamber containing
 143 buffered 40% formaldehyde preservative (which dilutes in the seawater to a concentration of
 144 about 4%, sufficient to fix and preserve the plankton). After each transect the CPR was
 145 transferred to a laboratory, where the samples were unloaded. The towed mesh was processed
 146 according to standard CPR protocols; first cut into separate samples (each representing 18.5 km
 147 of tow and about 3 m³ of seawater filtered) which were randomly apportioned amongst the
 148 analysts for plankton identification and counting. Every fourth oceanic sample was distributed
 149 for analysis with the remainder being archived, but over the Alaskan shelf consecutive samples
 150 were processed. The ship's log was used to determine the mid-point latitude and longitude of
 151 each sample (shown in Fig 1), along with the date and time.

152

153 **2.2 Taxonomic analysis**

154 As with all plankton samplers the CPR has biases. The mesh size is 270 μm and so organisms
 155 with dimensions smaller than this may not be quantitatively sampled, however, the effective
 156 mesh size may be much smaller depending on the abundance and morphology of plankton that

157 are caught (see Batten et al., 2003a for more details) and organisms such as coccolithophores
158 with a diameter of a few tens of microns are caught and identified. The formaldehyde
159 preservative used in the instrument does not fix naked dinoflagellates or ciliates so these groups
160 are not at all represented in the database. The sampling method can also result in damage to the
161 organisms so fragile groups, especially gelatinous plankton, may only be identifiable to a coarse
162 level.

163 There were four steps in analysing the plankton retained in a CPR sample. The first step was the
164 assessment of phytoplankton colour (the greenness of the sample, or Phytoplankton Colour
165 Index, PCI), which was determined by comparison with standard colour charts. This is a semi-
166 quantitative representation of the total phytoplankton biomass and includes the organisms that
167 are too fragile to survive the sampling process intact but which leave a stain on the mesh (Batten
168 et al., 2003b; Raitos et al., 2013). Hard-shelled phytoplankton were then semi-quantitatively
169 counted under a purpose-built microscope by viewing 20 fields of view (diameter 295 μm)
170 across each sample under high magnification (x 450) and recording the presence of all the taxa in
171 each field (presence in 20 fields is assumed to reflect a more abundant organism than presence in
172 2 fields for example). Small zooplankton were then identified and counted from a sub-sample by
173 tracking across the filtering mesh with the microscope objective (a 2 mm diameter field of view
174 = 2% of the sample width) whilst all zooplankton larger than about 2 mm were removed from the
175 mesh and counted, usually without sub-sampling. Identification in all cases was carried out to
176 the most detailed practicable taxonomic level and was a compromise between speed of analysis
177 and scientific interest. For example, since copepods make up the majority of the zooplankton
178 and remain mostly intact after sampling, most copepods were identified to species level whilst
179 rarer groups, or those not preserved well by the sampling mechanism (such as chaetognaths),
180 were identified to a lower level such as phylum. A list of taxa and their abundance in each
181 sample was thus generated, and from this summary indices (such as estimated zooplankton
182 biomass, total diatom abundance, etc.) were also calculated.

183 **2.3 Comparison of CPR Phytoplankton indices and satellite data.**

184 To compare the *in situ* phytoplankton seasonal cycles (PCI and diatoms from the CPR data) with
185 a satellite-derived ocean colour dataset, the monthly near-surface Chlorophyll-*a* (Chl-*a*) was
186 acquired from NASA's Oceancolor website (<http://oceancolor.gsfc.nasa.gov>). The Moderate-

187 resolution Imaging Spectroradiometer (MODIS on-board the Aqua platform) 4km resolution
188 Chl-*a* data were processed for the period 2003-2011 (O'Reilly et al., 2000). Standard NASA
189 algorithms were used for Chl-*a* (OC3) estimates; these are routinely processed by the Ocean
190 Biology Processing Group at the Goddard Space Flight Center (Feldman and McClain, 2012).
191 Using the monthly mean datasets, we constructed the area-averaged monthly climatologies.

192 Remotely sensed Chl-*a* data have known limitations especially in coastal, optically complex,
193 Case II waters where suspended sediments, particulate matter and/or dissolved organic matter do
194 not covary in a predictable manner with Chl-*a* (IOCCG 2000). For example, scattering by
195 sediments in turbid waters and underwater reflectance from shallow shelf regions may result in
196 relatively high water-leaving radiance in the near-infrared (NIR) wavelengths, which could
197 overestimate the correction term. For this reason satellite data from CI were excluded. Even so,
198 the Chl-*a* data used in the analysis may be influenced (generally resulting in an overestimation)
199 by the factors mentioned above, especially in the most coastal waters and/or very shallow waters
200 of the Alaskan Shelf area. However, the scope of the current study is to compare the general
201 variability of satellite-derived Chl-*a* and CPR phytoplankton in the Alaskan Shelf, regardless of
202 absolute concentrations. In addition, to gain confidence on the variability and pattern of satellite
203 derived Chl-*a*, we also compared the MODIS results with those from SeaWiFS. The area-
204 averaged monthly means, and the seasonal climatologies of the two satellite-derived Chl-*a*
205 datasets were significantly correlated ($r^2=0.78$, $p<0.0001$, and $r^2=0.98$, $p<0.0001$ respectively).

206

207 **2.4 Analysis of CPR plankton time series**

208 All shelf samples were extracted from the database. These samples were south of PWS 2000–
209 2003, and in CI and southeast of it 2004 to 2015 owing to the change in transect position.

210 **2.4.1 Abundance and seasonal timing**

211 The mean abundance per sampling event (monthly transects) was calculated for the entire shelf
212 region for various taxonomic groupings (e.g., total mesozooplankton, large copepod abundance,
213 large diatom abundance, dinoflagellates, etc). Mean seasonal cycles were calculated by
214 averaging the monthly averages for each month of the year (restricted to March to October).

215 Seasonal timing and annual abundance indices were calculated using a method proposed by
216 Grieve et al (2005) that relies on cumulative integration. In this case we integrated between day
217 60 and day 300 each year (assuming 0 abundance on days 60 and 300), and summed daily values
218 to give a cumulative total for the year. All years had 5-6 samplings, spaced at least monthly,
219 except 2003, 2008 and 2010 so these years should be treated with caution if data are shown. The
220 day of the year when 50% of the cumulative abundance occurred was calculated (this is the mid-
221 season, as an index of timing). An annual abundance anomaly (Log10, based on the geometric
222 mean of all years) was calculated for each year for the cumulative integrated biomass/abundance
223 at day 300.

224

225 2.4.2 Community composition

226 The same samples as described above were used but individual taxon abundances were extracted
227 to examine interannual variability in the taxa present. Data were divided into spring (April, May
228 and June) and late summer/autumn (August and September). Phytoplankton and
229 mesozooplankton were treated separately (microzooplankton were excluded). The mean annual
230 abundance of each taxon in each group (phyto or zooplankton, spring or autumn) was calculated
231 and then the data were transformed ($\text{Log}\{x + 1\}$) to reduce the impact of dominant taxa. Bray
232 Curtis dissimilarities were calculated for each pair of years, and then NMDS (in the SYSTAT
233 software package) used to display the ordinations in 2 dimensions.

234

235 2.4.3 Copepod community length

236 Size of its members is an important zooplankton community attribute, likely governing trophic
237 interactions. Change in size can only be accurately determined for the copepods captured by the
238 CPR as they are the only important and dominant group identified mostly to species. The
239 methodology of Richardson et al. (2006) was applied to the copepod counts. Mean copepod
240 community size (\bar{S}) for each sample was calculated:

241

242

$$\bar{S} = \frac{\sum_{i=1}^N (L_i \cdot X_i)}{\sum_{i=1}^N X_i}$$

243

244 Where L is the mid-range adult female total length (mm) per species (i) obtained from Chihara
245 and Murano (1997) and when not available, from Razouls et al. (2012), and X is its abundance.

246 Monthly means were calculated for the five warmest (2001, 2003, 2005, 2014 and 2015) and five
247 coldest years (2002, 2007, 2008, 2009 and 2012), based on the GAK1 dataset.

248 2.4.4 Physical data

249 In order to explain the patterns within the plankton data, time series of physical variables
250 were used. Temperature observations were available from the GAK1 dataset (location shown on
251 Fig 1), available at <http://www.ims.uaf.edu/gak1/>, which was the geographically closest source to
252 the CPR data of seasonally resolved *in situ* temperature. Monthly measurements have been made
253 at GAK 1 from 1970 to present from surface to depth. For this study, a mean of the four upper-
254 most water column measurements was calculated (0, 10, 20, and 30m) from each month to
255 represent water temperatures that most of the planktonic organisms would have experienced.
256 Where a month was not sampled in a particular year, the long term mean for that month was used
257 instead to create an unbroken time series of March to October values.

258 Some *in situ* temperature measurements were also available from a logger on the CPR
259 itself from 2000 to 2002 and 2011 to 2015. For each transect where a logger was fitted,
260 temperature was recorded every 5 minutes (15 minutes in 2000 to 2002) for the duration of the
261 tow. Data collected between 59°N and 60°N (2000-2002) or 57.5°N to 59°N (2011 onwards)
262 were averaged to represent temperature on the shelf at the depth of the CPR each sampled
263 month.

264 The CPR transect into Cook Inlet intersects with the outermost stations of the Seward Line (Fig
265 1). The mixed layer depth (MLD), an index of stratification (Potential Energy) and salinity
266 measurements were available from the Seward Line cruises in May of each year to provide
267 spring water column characteristics (the Seward Line is only sampled in May and

268 September/October so May was selected as best describing the conditions which might influence
269 the plankton through spring and summer when most of the CPR sampling occurred). A CTD
270 was deployed at each station and the MLD computed as the depth at which the density is greater
271 than 0.03kgm^{-3} at 5 m depth. The stratification parameter, the potential energy required to
272 redistribute the water-column mass by complete vertical mixing (J/m^3), was also
273 computed (Simpson et al., 1977). The thermocline is not necessarily fully established by the time
274 of the May cruise leading to variability along the line. We therefore averaged the values for all
275 stations to provide the best index of spring water column stability. Salinity data (from all depths)
276 were also available from all stations along the Seward Line.

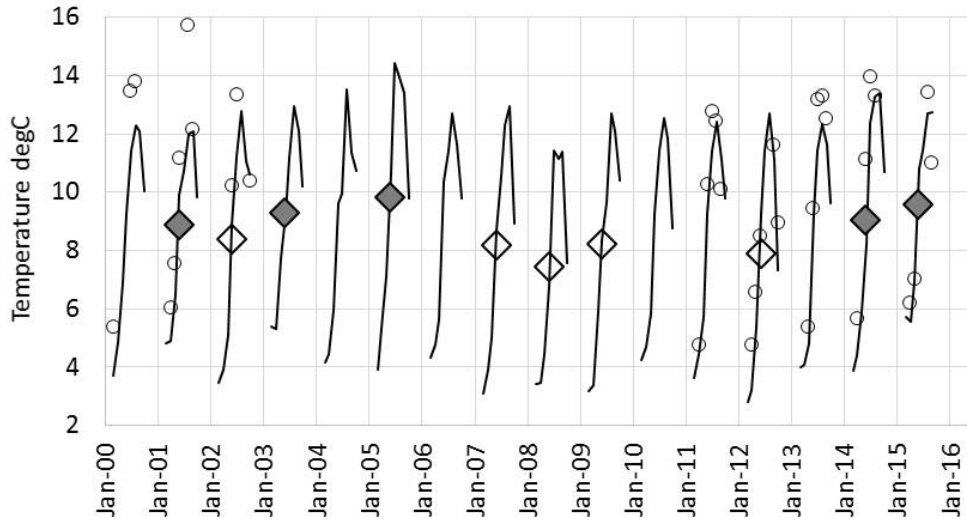
277

278 **3. Results**

279 **3.1. The physical environment**

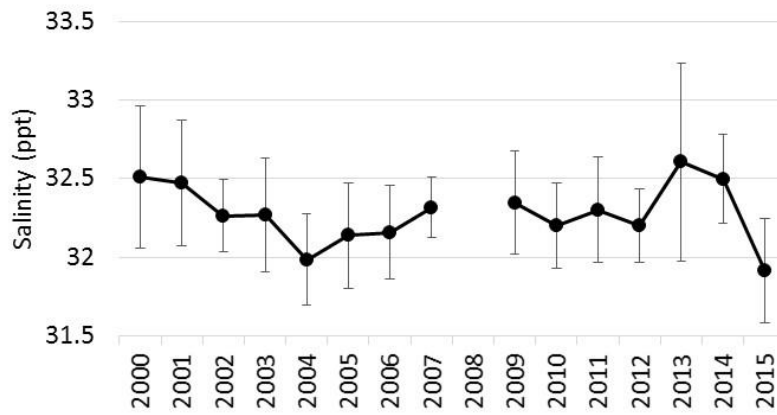
280 Physical data (SST, salinity, Potential Energy and Mixed Layer Depth) are shown in Fig 2. The
281 early part of the time series was relatively cool and then temperatures increased from 2003 to
282 2005. Another cool period followed, with 2008 being the coldest year of the record, before
283 temperatures rose in 2014 as the influence of the anomalous off-shore warming became apparent.
284 The time series ends with warm conditions resulting from the 2014 anomaly and the 2015 El
285 Niño. Salinities on the Seward Line stations in May each year were freshest in 2004 and 2015
286 (warm years, so likely some influence of early, or increased, snow melt) and most saline in 2000
287 and 2013 but note that outer stations were not sampled in 2008 (the coldest year). Water column
288 stability indices show that in the earlier warm period of 2004-05 the MLD was shallow and the
289 energy required to mix the water column was large (high Potential Energy), indicating stronger
290 stratification. While the colder period was missing data from 2008, 2007 showed a deeper MLD
291 and lower Potential Energy, suggesting weaker stratification. In the more recent warm period of
292 2014 and 2015 the MLD was shallow in 2014 but deeper in 2015 and the Potential Energy was
293 quite low in both years, suggesting quite weak stratification.

294



295

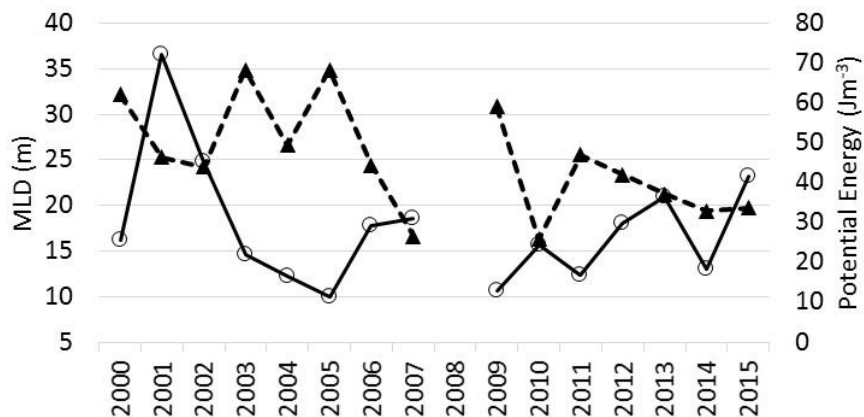
296 A.



297

298 B.

299



300

301 C.

302 Fig 2. Physical variables. Panel A. Mean monthly (Mar-Oct) SST from the GAK1 station
 303 (lines) and mean monthly *in situ* SST from loggers on the CPR (○). Filled diamonds
 304 indicate the mean annual (March-October) temperature for the 5 warmest years, unfilled
 305 diamonds indicate the mean for the 5 coldest years. Panel B. Salinity Data from May
 306 cruises on the Seward Line (error bars show st. dev.) Panel C. Water column stability
 307 shown by: solid line - mean Mixed Layer Depth, dashed line - mean Potential Energy.

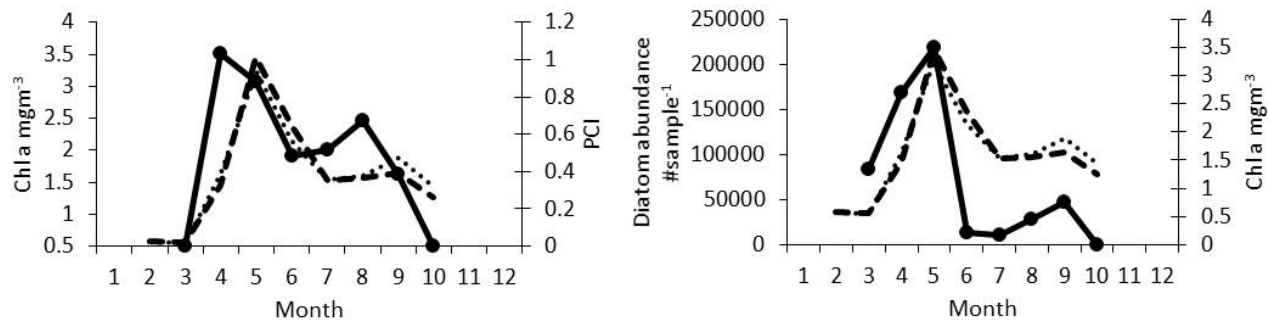
308

309 3.2 Abundance and seasonal timing

310 3.2.1 Phytoplankton

311 The phytoplankton counts from the CPR are not representative of the whole phytoplankton
 312 community, with a large mesh compared to most of the cells, and a preservative unsuitable for
 313 athecate cells; however, it is an internally consistent time series and larger and more robust
 314 phytoplankton are captured well. A comparison with satellite-derived chlorophyll-*a* data
 315 demonstrates that CPR phytoplankton data generate realistic seasonal cycles (Fig 3). The CPR
 316 PCI values peak on average one month earlier than the satellite measurements of chlorophyll-*a* in
 317 both the spring and autumn peaks, but the diatom abundances match the satellite-derived
 318 seasonal cycle very closely. The general pattern shows two diatom blooms; in spring and a lesser
 319 peak in late summer/autumn. This is typical of a shelf system where autumnal storms may
 320 increase mixing, bringing up nutrients and allowing a second phytoplankton bloom while light
 321 levels are sufficient. Thecate dinoflagellates are most abundant only in the summer and autumn

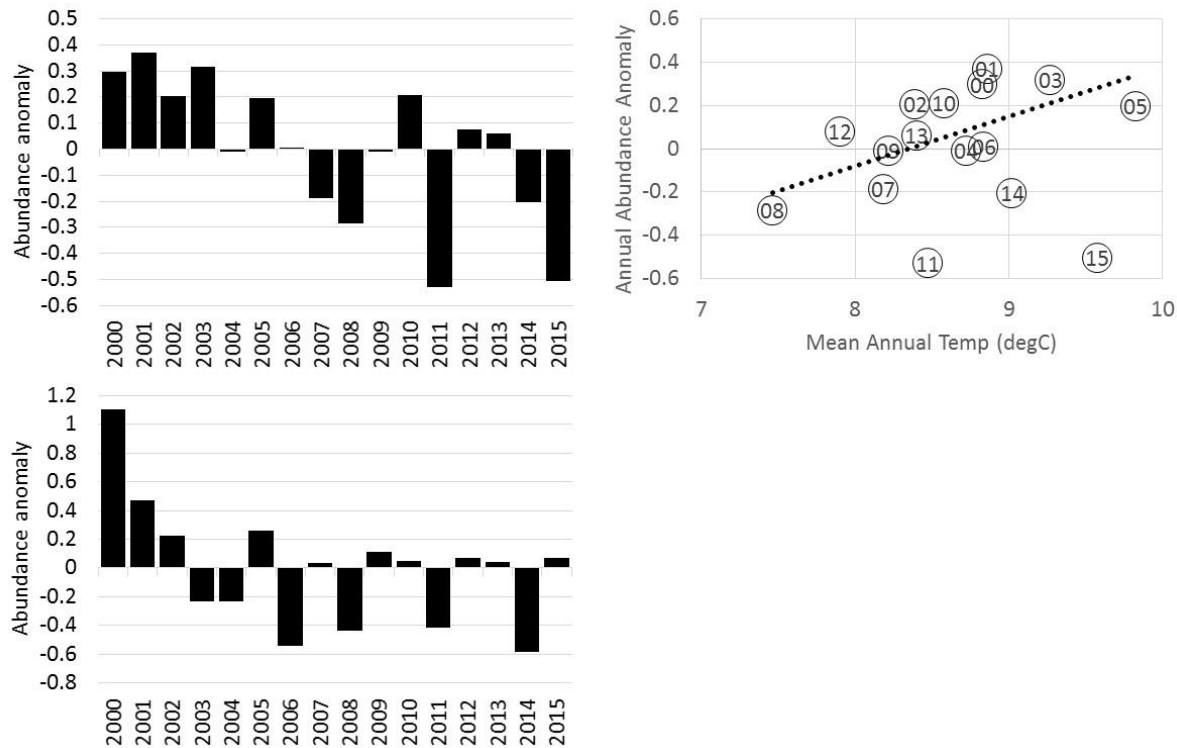
322 when waters are warmer. The PCI index closely follows the diatom cycle, but increases earlier
 323 (as evident in Fig 3 when compared with the satellite chlorophyll data). The difference between
 324 spring and autumn PCI is less than the difference between spring and autumn diatoms, perhaps
 325 because the index also incorporates a signal from the dinoflagellates.



326
 327 Figure 3. Mean monthly phytoplankton indices from CPR data (solid line, Phytoplankton
 328 Colour Index at left, diatom abundance at right) and satellite-derived chlorophyll-a (from
 329 MODIS, heavy dashed line and SeaWiFS, lighter dashed line on both graphs) for the
 330 region shown in Figure 1, excluding Cook Inlet.

331 Annual abundance anomalies of diatoms (calculated as previously described for March to
 332 October) are shown in Fig 4. During the first 14 years of the time series it was noted that there
 333 was a moderate, positive, significant correlation between diatom abundance and temperature
 334 ($r^2=0.28$, $p<0.05$ with either the annual mean GAK 1 temperature, or with the annual PDO index)
 335 with warm, PDO positive years having greater numbers of diatoms (Fig 4). However, 2014 and
 336 2015 did not follow this pattern and abundances were low, despite the very warm conditions.
 337 Numbers were also low in 2011 which was neither a warm nor cold year.

338



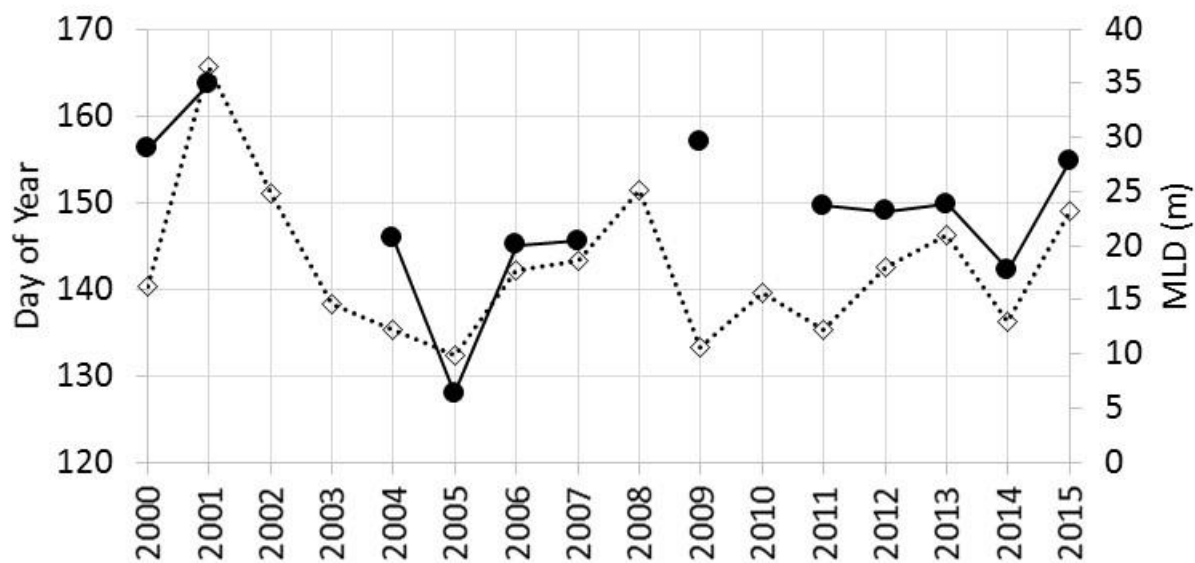
339

340 Figure 4. Annual abundance anomalies of diatoms (top left) and thecate dinoflagellates
 341 (bottom left). Right panel shows the relationship between diatom abundance and mean
 342 temperature (mean of March to October monthly GAK1 temperature). The dashed line
 343 indicates the relationship from 2000 to 2013 with year shown inside each data point.

344 Thecate dinoflagellates are numerically much less dominant than diatoms in CPR samples,
 345 ranging from between one third and one sixtieth of the diatom abundance. There were no
 346 significant relationships between the dinoflagellate mean annual abundance anomalies and
 347 physical variables, however, the linear decline through time is significant ($r^2=0.23$, $p<0.05$).
 348 This could be because of a regional difference as the region south of PWS, sampled only in
 349 2000–2003, had consistently higher abundances of dinoflagellates than the Cook Inlet and
 350 nearby shelf region sampled from 2004 and afterwards, however, since the two regions were not
 351 sampled simultaneously we cannot be certain. From 2004 onwards the pattern shows inter-
 352 annual variability with no trend.

353 Although the CPR sampling resolution is not sufficient to identify the exact timing of the spring
 354 phytoplankton bloom, we focused on just the spring diatom data, integrating abundances
 355 between days 60 and 180 (as described previously for the whole season) and taking the day of

356 the year where 75% of the spring diatom abundance was reached as an index of spring timing
 357 (years 2002, 2003, 2008 and 2010 were not sampled sufficiently often in the spring to calculate
 358 this index). There was no significant correlation between spring timing and temperature as
 359 indexed by mean annual GAK 1 temperature or the PDO (although 2005 and 2014 did have the
 360 earliest dates and the modest relationship was negative), however, the Seward Line MLD
 361 correlated significantly with diatom timing ($n=11$, $r^2=0.39$, $p<0.02$), so that in years with a
 362 greater MLD in May the spring peak was later (Fig 5). The correlation with potential energy of
 363 the water column was negative, but non-significant. There was also a significant correlation
 364 between diatom spring timing and the NPGO ($p<0.02$) so that with a positive NPGO (stronger
 365 westerly winds are associated with positive NPGO further south and through the shelf edge
 366 currents influence MLD in this region), the diatom peak is later.

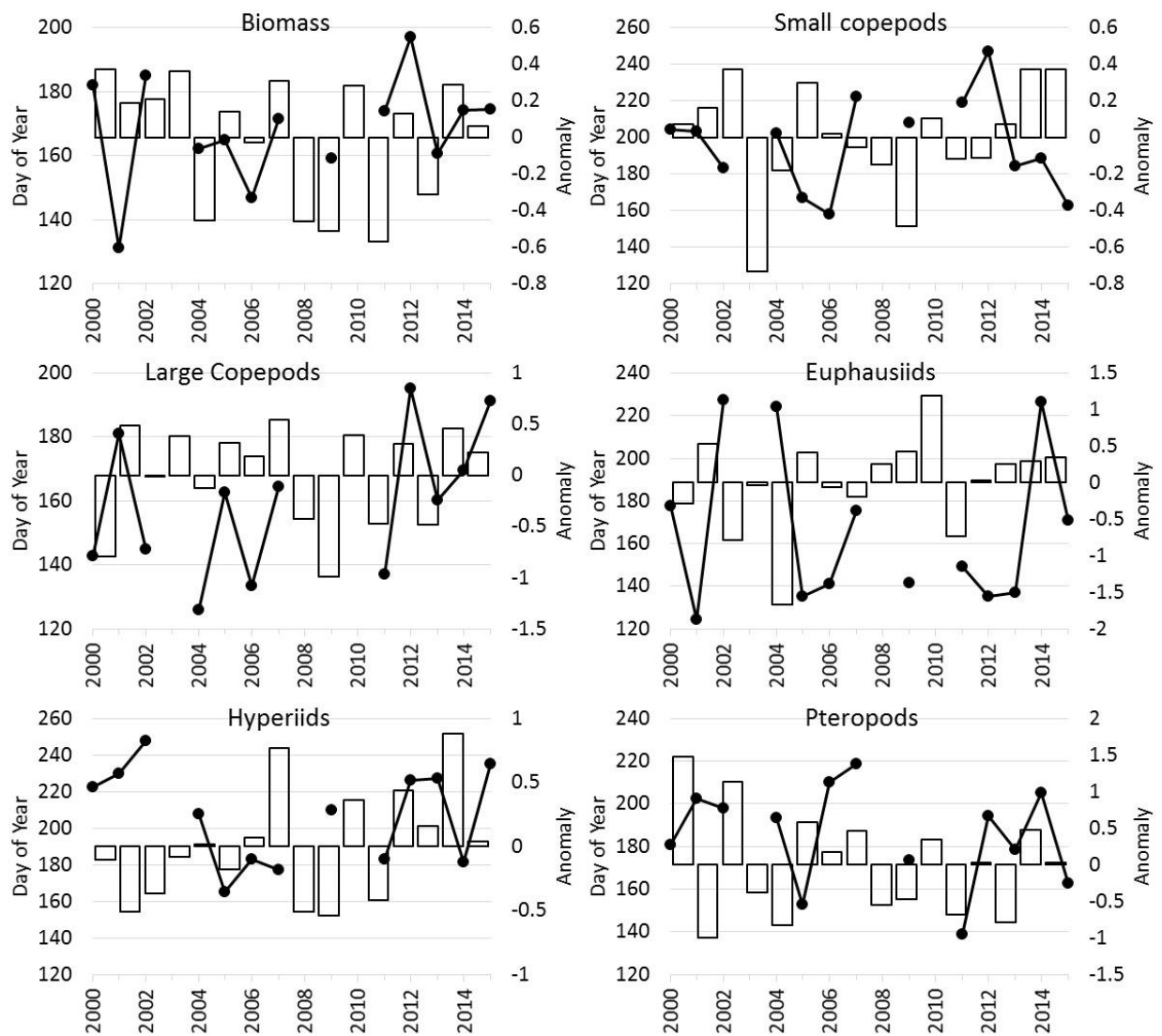


367
 368
 369 Figure 5. Spring diatom timing (day of year when 75% of the integrated daily abundance
 370 at day 180 was reached) for years when sampling resolution was sufficient (solid line),
 371 together with the time-series of mean May MLD along the Seward Line (dashed line).

372

373 3.2.2 Zooplankton

374 Estimated mesozooplankton biomass is a summary index of the overall zooplankton community,
 375 and the anomaly time series is shown in Fig 6, together with annual abundance anomalies of five
 376 of the dominant taxonomic groups (large copepods >2mm length, small copepods <2mm length,
 377 euphausiids, hyperiids, and pteropods). Also shown is an index of seasonal timing for each
 378 zooplankton variable, as day of the year when 50% of the integrated daily biomass/abundance
 379 was reached. No long term trends are evident in the time series, with the exception of hyperiid
 380 abundance which has generally increased over the 15 year period. Between-year variability is
 381 large in all six cases.



382
 383 Figure 6. Annual anomalies of zooplankton groups (bars) and seasonal timing (lines with
 384 dots). Top left panel shows total mesozooplankton biomass (estimated from taxonomic

385 abundance data, see methods). Other five panels show abundance anomalies for groups as
386 indicated; large copepods (length >2mm), small copepods (length < 2mm), euphausiids,
387 hyperiids, and pteropods.

388 There was a very strong positive correlation between the annual diatom abundance and
389 zooplankton biomass anomalies from 2000 to 2013 ($r^2=0.49$, $p<0.005$) so that years with a higher
390 abundance of diatoms had a higher zooplankton biomass, suggesting a trophic link. This
391 relationship was not present in 2014 and 2015 which had high zooplankton biomass but low
392 diatom abundance. All of the five major zooplankton taxonomic groups had positive correlations
393 between their abundance and diatom abundance until 2013, but none were individually
394 significant. Similarly, there were positive correlations between most of the zooplankton groups
395 and temperature, however, none were significant at the $p<0.05$ level. Temperature does,
396 however, have an effect on seasonal timing. The mid-point of the zooplankton biomass season is
397 later in cold years. This is also true for small and large copepods. For small copepods this is a
398 strong, negative relationship between seasonal timing and the PDO/temperature ($r^2=0.5$, $p=0.003$
399 with the PDO), but less so for large copepods ($r^2=0.2$, $p=0.09$) and for both groups the difference
400 in timing between the earliest and latest years was more than two months. There were no
401 significant relationships between euphausiids, hyperiids and pteropod seasonal timing and
402 temperature. To summarise; years with higher diatom abundance had higher zooplankton
403 biomass (at least until 2013), and in cold years the abundance of copepods was shifted later in
404 the year.

405

406 **3.3. Community composition**

407 83 phytoplankton taxa were recorded during the time series and 89 mesozooplankton taxa (eggs
408 and microplankton groups such as tintinnids and foraminifera were excluded). Table 2 shows
409 the most abundant 30 taxa for phytoplankton and zooplankton in spring and in late summer.
410 While many taxa are common to both seasons, their relative abundance does change (their
411 position in the table) and contributes to the community differences seen between seasons. Some
412 taxa are only abundant in one season; for example, dinoflagellates of the genus *Ceratium* are
413 more common in late summer and the large *Neocalanus* copepods are typically only found in

414 surface waters in spring. The MDS plots (Figs. 7 and 8) are 2 dimensional representations of the
 415 similarity of the spring or late summer/autumn communities between years (using all the taxa),
 416 so that years with the most similar communities in each treatment plot closest together. Stress
 417 values were moderately low, being between 0.12 and 0.17 for all analyses indicating that a two
 418 dimensional representation was appropriate.

419 Table 2. The 30 most abundant phytoplankton and zooplankton taxa occurring in each season.

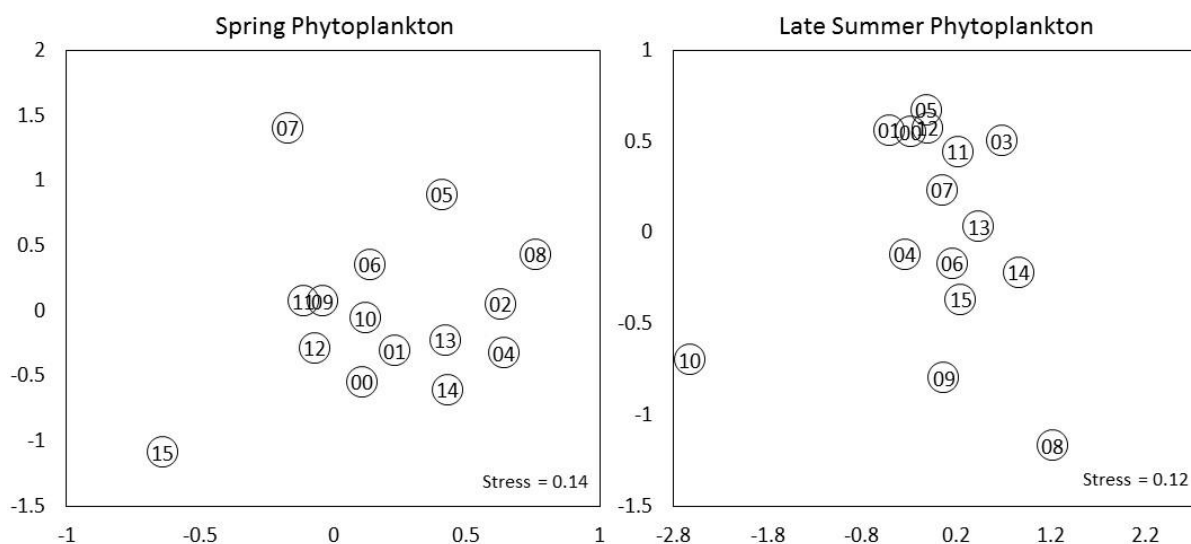
Phytoplankton, Spring	Phytoplankton, Late Summer	Zooplankton, Spring	Zooplankton, Late Summer
Thalassiosira spp.	Thalassionema nitzschioides	Pseudocalanus spp. C6	Pseudocalanus spp. C6
Chaetoceros spp. (Hyalochaetes)	Bacteriastrum spp.	Acartia longiremis	Acartia longiremis
Chaetoceros spp. (Phaeoceros)	Thalassiosira spp.	Calanus spp. C1-4	Echinoderm larvae
Corethron hystrix	Silicoflagellatae	cirripede larva	Calanus spp. C1-4
Thalassionema nitzschioides	Chaetoceros spp. (Hyalochaetes)	Neocalanus plumchrus C5	Oithona spp.
Silicoflagellatae	Chaetoceros spp. (Phaeoceros)	Echinoderm larvae	Acartia spp.
Neodenticula seminae	Pseudo-nitzschia seriata	Limacina helicina	Appendicularia
Unidentified Coscinodiscus spp.	Thalassiothrix longissima	Oithona spp.	Limacina helicina
Odontella aurita	Ceratium fusus	Euphausiacea calyptopis	Centropages abdominalis
Thalassiothrix longissima	Skeletonema costatum	Acartia spp.	Calanus pacificus C5-6
Rhizosolenia hebetata semispina	Rhizosolenia hebetata semispina	Neocalanus plumchrus/flemingeri C4	Euphausiacea calyptopis
Skeletonema costatum	Pseudo-nitzschia delicatissima complex	Appendicularia	Podon spp.
Pseudo-nitzschia delicatissima complex	Rhizosolenia setigera	Neocalanus plumchrus/flemingeri C2	Cirripede larva
Coccolithaceae	Detonula confervacea	Neocalanus flemingeri C5	Tortanus discaudatus
Rhizosolenia styliiformis	Ceratium lineatum	Cirripede nauplii	Clausocalanus spp.
Hyalochaete resting spore	Ditylum brightwellii	Euphausiacea	Calanus marshallae C5-6
Proboscia alata	Ceratium pentagonum	Calanus marshallae C5-6	Cyphonautes larva
Dinoflagellate cysts	Ceratium longipes	Clausocalanus spp.	Acartia danae
Ceratium pentagonum	Ceratium tripos	Decapoda larvae	Decapoda larvae
Pseudo-nitzschia seriata	Coscinodiscus spp.	Chaetognatha juveniles	Paracalanus spp. C6
Protoperidinium spp.	Coccolithaceae	Centropages abdominalis	Metridia pacifica C5-6
Stephanopyxis spp.	Biddulphia longicruris	Metridia spp. C1-4	Harpacticoida Total
Guinardia striata	Neodenticula seminae	Neocalanus cristatus C5-6	Chaetognatha juvenile
Cylindrotheca closterium	Pterosperma spp.	Neocalanus plumchrus/flemingeri C3	Euphausiacea
Ditylum brightwellii	Coscinodiscus concinnus	Cyphonautes larva	Neocalanus plumchrus/flemingeri C2
Detonula confervacea	Proboscia alata	Lamellibranch larvae	Hyperidea

Unidentified Nitzschia spp.	Hyalochaete resting spore	Eurytemora pacifica	Evadne spp.
Ceratium furca	Ceratium horridum	Hyperidea	Lamellibranch larvae
Ceratium horridum	Cylindrotheca closterium	Metridia pacifica C5-6	Ctenocalanus spp.
Paralia sulcata	Dinoflagellate cysts	Paracalanus spp. C6	Chaetognatha Adult

420

421 3.3.1 Phytoplankton

422 The MDS analyses in Fig 7 show no strong division between the two time periods of sampling,
 423 first adjacent to PWS (2000 to 2003) and then Cook Inlet from 2004 onwards (e.g., in the spring
 424 analysis 2002 plots closer to 2008 and 2013 than it does to 2000 or 2001 and the autumn analysis
 425 is similarly mixed). This suggests a similar phytoplankton community across the wider southern
 426 Alaska shelf (at least as the CPR sees it), likely a result of the distribution of plankton along the
 427 shelf by the Alaska Coastal Current.



428

429 Figure 7. Non-Metric Multidimensional Scaling analysis results of transformed spring
 430 (left, April to June) and late summer (right, August and September) phytoplankton
 431 taxonomic abundance data. The year is given in the centre of each point. Stress values for
 432 each ordination are given in the lower right.

433 In the spring analysis there is one main cluster with 3 years somewhat more distant and therefore
 434 dis-similar to other years; 2005, 2007, and 2015. The x-axis has little variability along it and the
 435 greater variability on the y-axis is likely related to temperature, with most of the warmer years

436 plotting negatively on this axis. The exception is 2005, however, if this year is removed the
437 relationship between temperature and the y-axis is significantly correlated ($r^2=0.40$, $p<0.01$).
438 2015 is quite distinct; as well as having generally low numbers of diatoms overall (Fig 4), there
439 were several taxa found for the first time in the region in spring 2015 (e.g. *Dactyliosolen*
440 *fragilissimus* and *Guinardia striata*) and some taxa commonly found in late summer but which
441 occurred in spring 2015 for the first time (*Bacteriastrum* spp, *Ceratium tripos*).

442 In the late summer/autumn analysis 2010 and 2008 plot distantly from other years and account
443 for the variability along the x-axis. The y-axis has years with higher numbers of dinoflagellates
444 (such as *Ceratium* spp.) plotting positively, and this axis is also positively correlated with
445 temperature ($p=0.07$) and potential energy ($p=0.06$). Dinoflagellates prefer warm, well-stratified
446 conditions.

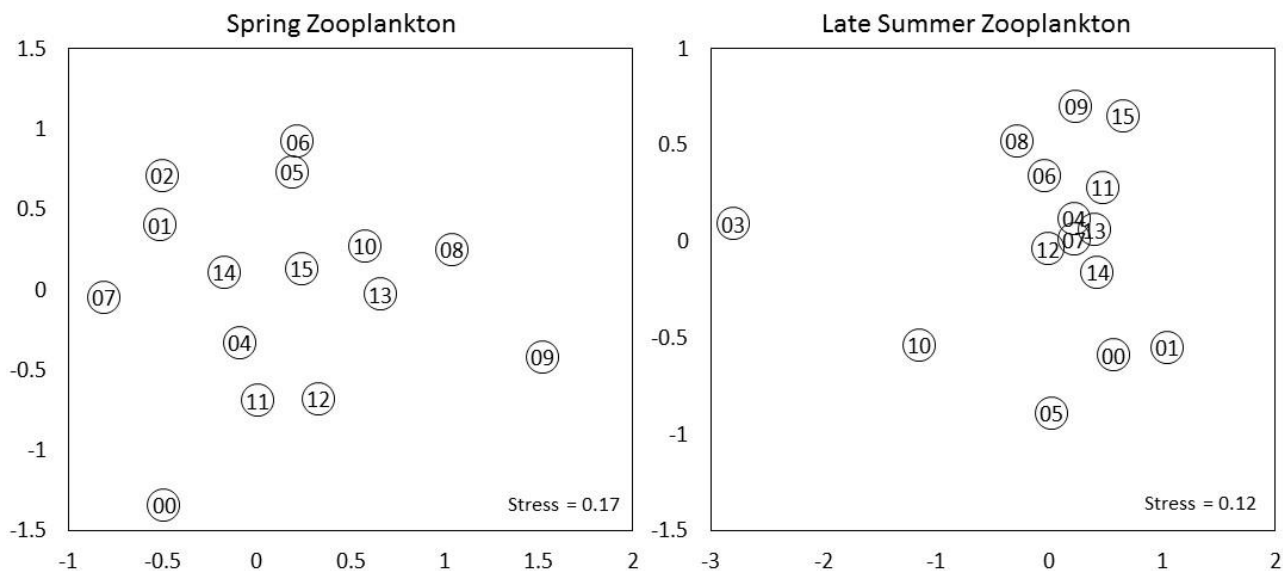
447 3.3.2 Zooplankton

448 The PWS shelf samples from 2000-2003 do not cluster separately from the 2004-2015 Cook
449 Inlet shelf samples in the zooplankton analyses either (Fig 8). In the spring analysis the years
450 2000 and 2009 appear to be different from other years, and different from each other.

451 Examination of the taxa showed that several copepod taxa were absent or in low abundance in
452 2000 and there were high numbers of pteropods in this year (also evident from the anomaly plots
453 in Fig. 6 where copepods were low in numbers and pteropods were high). The year 2009
454 contained some occurrences of rarer taxa such as *Paraeuchaeta* spp., sergestids and higher
455 numbers of appendicularians. These taxa were present in some other years, but their combined
456 effects influenced the overall difference in 2009 community composition. There were no strong
457 relationships between the axes and physical variables. The y-axis of the spring plot is likely
458 related to the PDO/temperature with PDO positive, warm years mostly positive on this axis.
459 2008 is, however, in the centre and not as negative as might be expected if this relationship was a
460 significant driver.

461 The late summer analysis has several years near the lower half of the plot that are dis-similar to
462 the main cluster with 2003 standing out as particularly distinct. Many taxa were absent in this
463 year and two copepod taxa, *Epilabidocera* spp. and *Centropages abdominalis* were relatively
464 abundant. The y-axis of this plot relates strongly to the abundance of diatoms. Years with a

465 positive diatom anomaly plot negatively on the y-axis while years with low numbers of diatoms
 466 are near the top ($r^2=0.44$, $p<0.01$) suggesting a relationship between phytoplankton abundance
 467 and zooplankton community structure.



468

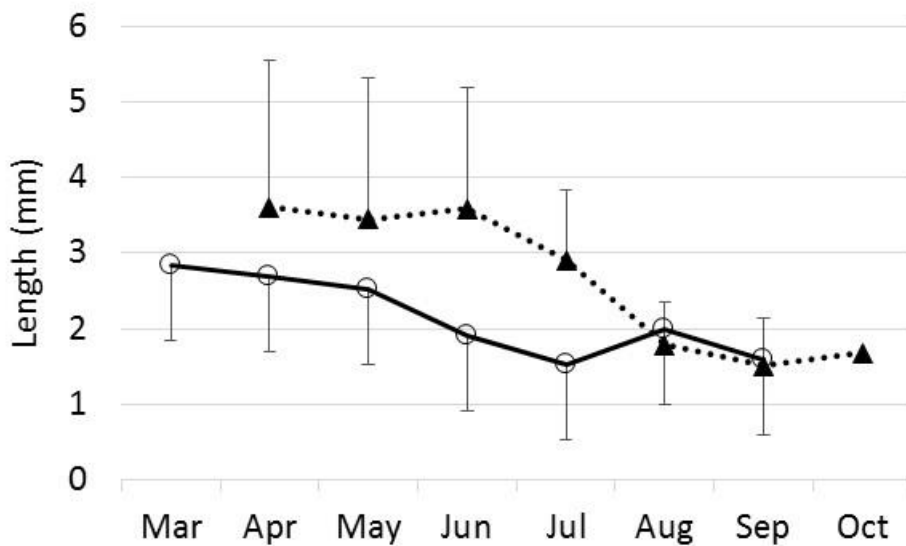
469 Figure 8. Non-Metric Multidimensional Scaling analysis results of transformed spring
 470 (left, April to June) and late summer (right, August and September) zooplankton
 471 taxonomic abundance data. The year is given in the centre of each point. Stress values for
 472 each ordination are given in the lower right.

473

474 3.3.3. Copepod community size

475 A total of 43 copepod taxa were recorded, ranging from individual stages in the case of the
 476 dominant species *Neocalanus plumchrus* (stages C2 to C6 were separately counted, though
 477 adults were rare) to genus level for those species more difficult to distinguish such as *Oithona*
 478 spp. The dominant taxa are shown in Table 2. The seasonal cycle of copepod community size, or
 479 the mean length of copepods in the community as represented by adult female length, (CCS) is
 480 shown in Fig. 9 and reveals the expected pattern where large copepods are more prevalent earlier
 481 in spring and, as these species descend to diapause in summer, the community becomes
 482 dominated by smaller species reducing the CCS, as reported in Coyle and Pinchuk (2003). The
 483 influence of temperature on the copepod community is clear, however, with the group of 5

484 warmest years having significantly smaller mean CCS in all spring and early summer months
 485 than the group of 5 coldest years (t -test, $p < 0.05$ for April and May, $p < 0.0001$ for June and July).
 486 Smaller species are both more numerous in warm than in cold years and have an earlier seasonal
 487 cycle, both factors contributing to a lower CCS in warm years. In August and September there
 488 was no significant difference in CCS between groups of years since even in cold years large
 489 *Neocalanus* copepods have almost all entered diapause by this time and the community is always
 490 dominated by smaller species such as *Acartia*, *Pseudocalanus* and *Paracalanus* spp.



491
 492 Figure 9. Monthly mean copepod length (mean Copepod Community Size, see methods
 493 section for derivation) for the 5 warmest years (solid line with circles) and the 5 coldest years
 494 (dashed line with triangles). Error bars show standard deviation (in one direction only to
 495 avoid clutter).

496
 497 **4. Discussion**

498 Our analyses have treated the shelf as one water body, which is an over-simplification since
 499 influences of the various current systems which run along the shelf will likely be different on the
 500 inner versus the outer shelf. The large scale resolution of CPR sampling (each sample covers
 501 18.5 km) is some mitigation for this approach. Where whole-shelf temperature data from the
 502 CPR logger are available (Fig 2, section 3.1) they show the same broad inter-annual patterns as

503 the GAK1 time series but this is only part of the story. Horizontal temperature gradients on the
504 Gulf of Alaska shelf are weak compared to salinity gradients but there are, however, cross-shelf
505 gradients in stratification. In spring, the inner half of the shelf stratifies primarily due to salinity
506 and is thus affected by the magnitude and/or timing of winter and spring runoff (Janout et al.
507 2010). In contrast, the onset of springtime stratification over the outer half of the shelf is
508 controlled by vertical temperature gradients. However, anomalously weak down-welling (or
509 upwelling-favorable) winds can spread low-salinity waters over the outer shelf and thereby affect
510 the stratification here meaning salinity variability has a strong influence on water column
511 structure across the entire shelf (Weingartner et al., 2002). We may therefore expect climate
512 forcing which influences the timing and intensity of freshwater run-off from the surrounding
513 watersheds to have a large influence on the plankton. Temperature variability will also impact
514 lower trophic levels directly in a number of ways; via basic metabolic processes with
515 temperature-dependent rates and for at least some species the timing of life history events is
516 related to ambient temperature (e.g. Batten et al., 2003c). We would therefore expect physical
517 processes which create variability in either, or both, freshwater and heat content of the Alaskan
518 Shelf waters to lead to variability in the plankton communities there.

519 Although the CPR was not designed as a phytoplankton sampler, and the mesh size is larger than
520 many phytoplankton cells, there are nonetheless valuable insights into phytoplankton variability
521 that can be gained from CPR data, because it is an internally consistent sampler and does retain a
522 representative proportion of even quite small cells (especially if chain-forming). Figure 3,
523 section 3.2.1 demonstrates that seasonal cycles derived from the CPR data closely replicate those
524 seen from satellites for the same area, confirming that useful information can be gained.
525 Through the first 14 years of the time series of CPR sampling on the Alaskan Shelf we have
526 found that warm years had generally higher abundances of the larger cells retained by the CPR,
527 particularly of diatoms (Fig. 4). The diatom anomaly time series has some similarity to a
528 chlorophyll-*a* anomaly time series derived from satellite measurements for a wider area of the
529 coastal Gulf of Alaska (Waite and Mueter, 2013). Their time series showed positive anomalies
530 from 1998 to 2002, negative anomalies from 2003 to 2005, close to average for 2006 to 2010,
531 and strongly negative in 2011. The CPR diatom anomalies were high in the early years also,
532 suggesting a widespread event, and the decline in the middle years was probably not related to
533 the change in time series location since the Waite and Mueter study showed a similar decline in

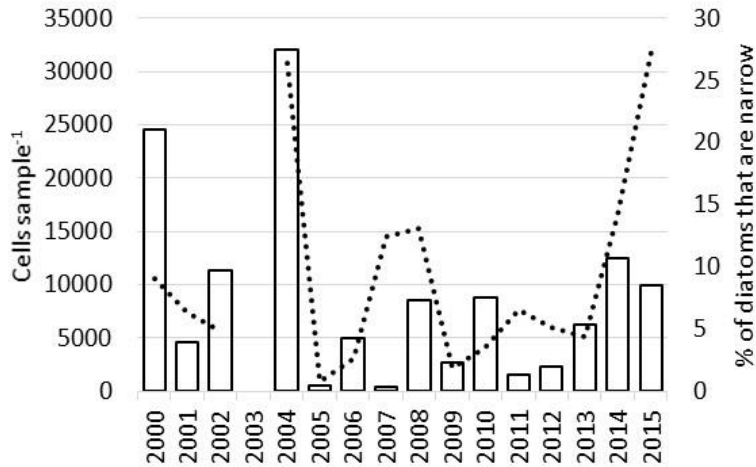
534 chlorophyll-*a* at this time. The strongly negative anomaly in 2011 was common to both studies.
535 Causes of this low productivity year are still being explored, however, the CPR zooplankton data
536 show that the effects passed up the food chain from the phytoplankton; zooplankton biomass had
537 the lowest anomaly of the time series to date in 2011 (Fig. 6). Interestingly, the community
538 composition analyses did not identify 2011 as an anomalous year (Figs 7 and 8). In terms of the
539 type of taxa present and their relative abundance, 2011 was quite similar to several other years.

540 Diatom spring timing revealed an influence of water column conditions (Fig. 5). We might
541 expect temperature to have a direct effect on diatom timing but this was not apparent, instead it
542 was the degree of water column stability in May that provided the influence with a less stable
543 water column (particularly a deeper MLD and to a lesser extent the lower potential energy)
544 having a later spring peak in diatoms. There was also a significant correlation with the NPGO
545 index, which is known to explain salinity variability further south in the California Current
546 system (DiLorenzo *et al.*, 2008). The NPGO reflects both regional and basin scale variations in
547 wind-driven circulation and advection processes. The relationships between the diatom timing
548 and MLD and NPGO emphasises that phytoplankton processes are very much dependent on the
549 physical oceanographic conditions.

550 Hard-shelled dinoflagellates are numerically much less important than the diatoms, typically
551 having an abundance one tenth that of the diatoms in the CPR data, so the decline over time seen
552 in Figure 4 is not likely to have had much influence on total phytoplankton biomass. It has,
553 however, contributed to the changing phytoplankton community composition shown in Figure 7
554 by influencing the late summer composition, when dinoflagellates are typically most abundant.
555 The NMDS analysis also showed an influence of the spring stratification strength (potential
556 energy, shown in Fig 2.) on summer phytoplankton composition. While stratification data from
557 summer would be desirable to examine this further, it is feasible that the water column stability
558 measured in late spring (May) would influence the community structure in the late summer,
559 especially the numbers and types of dinoflagellates that prefer well-stratified waters.

560 Total mesozooplankton biomass was strongly positively correlated with diatom abundance for
561 the years 2000-2013. The CPR data up to 2013 support the hypothesis that the physical
562 environment of the Gulf of Alaska shelf (temperature and water column stability) influences the
563 phytoplankton (diatom abundance and timing, dinoflagellate abundance), which in turn controls

564 the quantity of mesozooplankton. However, these relationships were not apparent in the warm
565 years of 2014 and 2015 when diatoms were unexpectedly low, in what has been termed a
566 “marine heatwave” (DiLorenzo and Mantua, 2016) influenced first by the anomaly known as the
567 Blob (Bond et al., 2015) and then an El Niño in 2015. These two years had the highest numbers
568 of small copepods recorded in the time series which also were biased earlier in the year than
569 average (Fig 6). It is possible that the data for these two years show top-down control of the large
570 diatoms by copepod grazing pressure, which was not seen in other warm years with high diatoms
571 and high zooplankton abundance/biomass such as 2005. It is unlikely that the higher
572 temperatures caused a non-linear response of lower productivity in the diatoms since these
573 species also occur further south where such temperatures are normal. An alternative explanation
574 is that the unusual conditions caused an unfavourable nutrient regime which reduced the
575 productivity of large diatoms. The taxa recorded by the CPR in spring 2014 and 2015 did show a
576 bias towards diatoms with longer, narrow cells (e.g. *Proboscia* spp., *Thalassiothrix* spp. and
577 pennate species). Figure 10 shows that only 2004 had a similarly high proportion of such cells
578 and the spring community composition analyses also show 2004 and 2014 as very similar. Cells
579 with this narrow morphology have a high surface area to volume ratio which would facilitate the
580 take-up of nutrients; studies have shown that smaller cells which also have a higher SA:Vol take
581 up nutrients faster (Friebele et al., 1977, Geider et al., 1986). If nutrients were scarce they would
582 have an advantage over the rounder cell types. However, the stratification indices shown in Fig.
583 2 do not suggest that 2014 and 2015 were especially stratified which might have limited the
584 nutrients introduced by mixing. In 2015 there was an even higher proportion of these narrow
585 cells, with low diatoms overall and high numbers of copepods still. The years 2014 and 2015
586 were also the only years of the time series when no coccolithophores were recorded in the
587 samples, so other as yet unknown factors that influence phytoplankton community structure were
588 also in play. It is also clear that the high numbers of copepods in these years must have been
589 eating something, if not the large diatoms then some part of the plankton community not well
590 resolved by the CPR.



591

592 Figure 10. Bars show the number of narrow, long diatom cells in spring of each year
 593 (April-June) while the dashed line shows the proportion of the total diatom community
 594 that they represent.

595 Copepod seasonal timing is dependent on temperature since copepods are poikilothermic and
 596 their metabolic processes, including development rate, are faster in warm conditions (see Batten
 597 *et al.*, 2003c and Mackas *et al.*, 2009). The index of season mid-point calculated here ranged
 598 from day 126 to day 200 for large copepods, and day 163 to day 247 for small copepods. This is
 599 a considerable amount of variability – over 2 months in each case, and could potentially impact
 600 larger predators that time their reproduction or migration to take advantage of a peak in their
 601 prey. Zooplankton community composition was also likely influenced by temperature (Fig. 8
 602 and section 3.3.2). These changes were not as dramatic as a replacement of many species by
 603 others, rather a change in relative abundances with temporary occurrences of some rare species
 604 (*e.g.*, the copepod *Acartia danae*, usually found below 40°N but found in the CPR samples from
 605 the Alaskan shelf in the warm years 2005 and 2015). CPR data from the oceanic NE Pacific
 606 have noted the northwards extension of warm water species to the GOA in the warmest years of
 607 the last decade (Batten and Walne, 2011) and Hopcroft *et al.* (2007) report a seasonal ingress of
 608 southern species along the Seward Line also in the warm year 2005. As well as warm water
 609 species occurring, there is also a shift towards a smaller mean size of copepod (Fig 9 and section
 610 3.3.3) through increased productivity of smaller species (which have multiple generations in one
 611 year) and an earlier increase in numbers. If smaller and/or warm water species contribute a
 612 significant amount to the zooplankton populations, they could present a dietary challenge to

613 zooplankton predators assuming their nutritional quality varies from the more typical subarctic
614 diet.

615 In summary, we have documented interannual variability in concentration and composition of
616 the plankton community of the region over a 16 year time period. At least in part and suggested
617 by correlative relationships, this variability can be attributed to changes in the physical
618 environment, particularly temperature and its direct effects on metabolic processes as well as
619 indirect effects on water column stability. The study ends with two anomalous years (2014 and
620 2015) for which previous relationships between temperature, diatom abundance and small
621 copepod abundance under warm conditions do not hold. The unusual warmth also continued into
622 2016 and impacts on the plankton communities from such sustained anomalous conditions
623 remains unknown. The CPR continues to sample the Alaskan Shelf and given the rapidly
624 changing climate the importance of regular, consistent sampling cannot be over-emphasised.

625

626 **Acknowledgements**

627 The authors are grateful to the officers and crew of the Matson (formerly Horizon) Kodiak which
628 has sampled this transect for over 12 years and to Matson and Horizon Shipping for their
629 voluntary involvement with the project. Funding for this study was provided by the North Pacific
630 CPR Consortium, which comprises the Exxon Valdez Oil Spill Trustee Council (currently via its
631 long-term monitoring program, GulfWatchAlaska), the North Pacific Research Board through
632 project number 1001, the Canadian Department of Fisheries and Oceans, Sir Alister Hardy
633 Foundation for Ocean Science and the North Pacific Marine Science Organisation. The research
634 described in this paper was supported by the Exxon Valdez Oil Spill Trustee Council. However,
635 the findings and conclusions presented by the author(s) are their own and do not necessarily
636 reflect the views or position of the Trustee Council. Thanks to Kinnetic Laboratories and Mr,
637 Doug Moore for preparing the equipment and samples, Dr Tom Weingartner, Dr Scott Pegau and
638 three anonymous reviewers provided valuable comments which improved this manuscript. This is
639 NPRB publication #***.

640

641 **Literature Cited**

- 642 Batten, S.D and Walne, A.W. (2011) Variability in northwards extension of warm water
643 copepods in the NE Pacific. *Journal of Plankton Research*, 33, 1643-1653.
- 644 Batten, S.D., Clarke, R.A., Flinkman, J., Hays, G.C., John, E.H., John, A.W.G., Jonas, T.J.,
645 Lindley, J.A., Stevens, D.P., Walne, A.W. (2003a) CPR sampling – The technical
646 background, materials and methods, consistency and comparability. *Progress in*
647 *Oceanography*, 58, 193-215.
- 648 Batten, S.D., Walne, A.W., Edwards, M. and Groom, S. B. (2003b) Phytoplankton biomass from
649 Continuous Plankton Recorder data: An assessment of the phytoplankton colour index.
650 *Journal of Plankton Research*, 25, 697-702.
- 651 Batten, S.D., Welch, D.W., and Jonas, T. (2003c) Latitudinal differences in the duration of
652 development of *Neocalanus plumchrus* copepodites. *Fisheries Oceanography*, 12(3), 201-208.
- 653 Bond, N. A., M. F. Cronin, H. Freeland, and N. Mantua (2015) Causes and impacts of the 2014
654 warm anomaly in the NE Pacific. *Geophysical Research Letters*, 42, 3414–3420. DOI:
655 10.1002/2015GL063306.
- 656 Chihara M, Murano M (Eds.) (1997) An illustrated guide to marine plankton in Japan. Tokai
657 University Press, Tokyo, p 1574. ISBN 4486012895.
- 658 Cooney, R.T., Coyle, K.O., Stockmar, E. and Stark, C, (2001) Seasonality in surface-layer net
659 zooplankton communities in Prince William Sound, Alaska. *Fisheries Oceanography*, 10,
660 97-109.
- 661
- 662 Coyle, K.O. and Pinchuk, A.I. (2003) Annual cycle of zooplankton abundance, biomass and
663 production on the northern Gulf of Alaska shelf, October 1997 through October 2000.
664 *Fisheries Oceanography*, 12 327-338.
- 665
- 666 DiLorenzo, E., and Mantua, N. (2016) Multi-year persistence of the 2014/15 North Pacific
667 marine heatwave. *Nature Climate Change*, published online:11 July 2016 DOI:10.1038/
668 nclimate3082.

669 Di Lorenzo E., Schneider N., Cobb K. M., Chhak, K., Franks P. J. S., Miller A. J., McWilliams J.
670 C., Bograd S. J., Arango H., Curchister E., Powell, T. M. and Rivere, P. (2008) North Pacific
671 Gyre Oscillation links ocean climate and ecosystem change. *Geophysical Research Letters*,
672 35, L08607, doi:10.1029/2007GL032838.

673 Exxon Valdez Oil Spill Trustee Council (2010) Exxon Valdez Oil Spill Restoration Plan: 2010
674 Update of injured resources and services. May 2010. EVOS Trustee Council, Anchorage,
675 Alaska, 48 pages. Available at
676 <http://www.evostc.state.ak.us/Universal/Documents/Publications/2010IRSUpdate.pdf>

677 Feldman, G. C., and C. R. McClain (2012) Ocean Color Web, MODIS Reprocessing R2009,
678 edited by N. Kuring and S. W. Bailey, <http://oceancolor.gsfc.nasa.gov>, NASA Goddard
679 Space Flight Center.

680 Francis, R. C. and Hare, S.R. (1994) Decadal-scale regime shifts in the large marine ecosystems
681 of the Northeast Pacific: a case for historical science. *Fisheries Oceanography* 3: 279-291.

682 Friebele, E.S., Correll, D.L. & Faust, M.A. (1978) Relationship between phytoplankton cell size
683 and the rate of orthophosphate uptake: *in situ* observations of an estuarine population. *Marine*
684 *Biology*. 45: 39-52.

685 Geider, R.J., Platt, T., and Raven, J.A. (1986) Size dependence of growth and photosynthesis in
686 diatoms: a synthesis. *Marine Ecology Progress Series*, 30; 93-104.

687 Grieve W, Prinage S, Zidowitz H, Nast J, Reiners F (2005) On the phenology of North Sea
688 ichthyoplankton. *ICES Journal of Marine Science* 62:1216 - 1223.

689 Hopcroft, R., Coyle, K., Weingartner, T. and Whitley, T. (2007) Gulf of Alaska Long-term
690 Observations: the Seward Line. Final report to the North Pacific Research Board, Dec 2007.

691 IOCCG (2000), Remote Sensing of Ocean Colour in Coastal, and Other Optically-Complex
692 Waters *Rep. No. 3 IOCCG*, Dartmouth, Canada.

693 Janout, M.A., Weingartner, T.J., Royer, T.C. and Danielson, S.L. (2010) On the nature of winter
694 cooling and the recent temperature shift on the northern Gulf of Alaska shelf. *Journal of*
695 *Geophysical Research: Oceans*, 115, 2156-2202.

696 Ladd, C., N. B. Kachel, C. W. Mordy, and P. J. Stabeno (2005) Observations from a Yakutat
697 eddy in the northern Gulf of Alaska, *Journal of Geophysical Research: Oceans*, 110,
698 C03003, doi: 03010.01029/02004JC002710.

699

700 Mackas, D.L., Batten, S.D., and Trudel, M. (2007) Effects on zooplankton of a warming ocean:
701 recent evidence from the Northeast Pacific. *Progress in Oceanography*, 75, 223-252.

702 Mantua, N.J., S.R. Hare, Y. Zhang, J.M. Wallace, and R.C. Francis, (1997) A Pacific decadal
703 climate oscillation with impacts on salmon. *Bulletin of the American Meteorological*
704 *Society*, Vol. 78, pp 1069-1079

705

706 Mueter, F.J., Broms, C., Drinkwater, K.F., Friedland, K.D., Hare, J.A., Hunt, G.L., Webjorn, M.,
707 and Taylor, M. (2009) Ecosystem responses to recent oceanographic variability in high-
708 latitude Northern hemisphere ecosystems. *Progress in Oceanography*, 81, 93-110.

709

710 Okkonen, S.R., Weingartner, T.J., Danielson, S.L., and Musgrave, D.L. (2003) Satellite and
711 hydrographic observations of eddy-induced shelf-slope exchange in the northwestern Gulf of
712 Alaska. *Journal of Geophysical Research*, 108 (C2), 3033, doi:10.1029/2002JC001342.

713 O' Reilly, J. E., et al. (Eds.) (2000), *SeaWiFS Postlaunch Calibration and Validation Analyses,*
714 *Part 3*, NASA Goddard Space Flight Centre, Greenbelt, Maryland.

715 Raitos, D.E., Walne, A., Lavender, S.J., Licandro, P., Reid, P.C., and Edwards, M. (2013) A 60-
716 year ocean colour data set from the Continuous Plankton Recorder. *Journal of Plankton*
717 *Research*, 35(1): 158–164

718 Razouls, C., de Bovée, F., Kouwenberg, J., and Desreumaux, N. 2005-2012. - Diversity and
719 Geographic Distribution of Marine Planktonic Copepods. Available at [http://copepodes.obs-](http://copepodes.obs-banyuls.fr/en)
720 [banyuls.fr/en](http://copepodes.obs-banyuls.fr/en).

721 Richardson, A.J., Walne, A.W., John, A.W.G.J., Jonas, T.D., Lindley, J.A, Sims, D.W., Stevens, D.,
722 and Witt, M. (2006) Using continuous plankton recorder data. *Progress in Oceanography*, 68,
723 27-74.

724 Royer, T.C., (1979) On the effect of precipitation and runoff on coastal circulation in the Gulf of
725 Alaska. *Journal of Physical Oceanography*, 9, 555–563.

726 Simpson, J. H., Hughes, D. H., and Morris, N. C. G. (1977) The relation of the seasonal
727 stratification to tidal mixing on the continental shelf. A voyage of discovery. George Deacon
728 70th anniversary volume (ed. Angel, MV) Pergamon, London, 327-340.

729 Stabeno, P.J., Bond, N.A., Hermann, A.J., Kachel, N.B., Mordy, C.W. and Overland, J.E. (2004)
730 Meteorology and oceanography of the Northern Gulf of Alaska, *Continental Shelf Research*,
731 24, 859-897.

732 Waite, J.N. and Mueter, F.J (2013) Spatial and temporal variability of chlorophyll-a
733 concentrations in the coastal Gulf of Alaska, 1998-2011, using cloud-free reconstructions of
734 SeaWiFS and MODIS-Aqua data. *Progress in Oceanography*, 116, 179-192.

735 Weingartner, T.J., Danielson, S.L. and Royer, T.C. (2005) Freshwater variability and
736 predictability in the Alaska Coastal Current, *Deep Sea Research Part II: Topical Studies in*
737 *Oceanography*, 52, 169-191.

738 Weingartner, T. J., K. O. Coyle, B. Finney, R. Hopcroft, T. Whitley, R. D. Brodeur, M. Dagg,
739 E. Farley, D. Haidvogel, L. Halderson, A. Herman, S. Hinckley, J. M. Napp, P. J. Stabeno, T.
740 Kline, C. Lee, E. Lessard, T. Royer, S. Strom. (2002). The Northeast Pacific GLOBEC
741 Program: Coastal Gulf of Alaska. *Oceanography*, 15:48-63